6064–6073 *Nucleic Acids Research, 2017, Vol. 45, No. 10* *Published online 28 February 2017*
doi: 10.1093/nar/gkx149

AUF1 facilitates microRNA-mediated gene silencing

Kyung-Won Min[1,†], Myung Hyun Jo[2,†], Soochul Shin[2,†], Sylvia Davila[1], Richard W. Zealy[1], Soo Im Kang[3], Lawson T. Lloyd[1], Sungchul Hohng[2,*] and Je-Hyun Yoon[1,4,*]

[1]Department of Biochemistry and Molecular Biology, Medical University of South Carolina, Charleston, SC 29425, USA, [2]Department of Physics and Astronomy, Institute of Applied Physics, National Center for Creative Research Initiatives, Seoul National University, Seoul 151-747, Korea, [3]Department of Plastic Surgery, Seoul National University Bundang Hospital, Seongnam 13605, Korea and [4]Laboratory of Genetics, National Institute on Aging-Intramural Research Program, NIH, Baltimore, MD 21224, USA

Received May 18, 2016; Revised February 17, 2017; Editorial Decision February 20, 2017; Accepted February 21, 2017

ABSTRACT

Eukaryotic mRNA decay is tightly modulated by RNA-binding proteins (RBPs) and microRNAs (miRNAs). RBP AU-binding factor 1 (AUF1) has four isoforms resulting from alternative splicing and is critical for miRNA-mediated gene silencing with a distinct preference of target miRNAs. Previously, we have shown that AUF1 facilitates miRNA loading to Argonaute 2 (AGO2), the catalytic component of the RNA-induced silencing complex. Here, we further demonstrate that depletion of AUF1 abolishes the global interaction of miRNAs and AGO2. Single-molecule analysis revealed that AUF1 slowed down assembly of AGO2–let-7b–mRNA complex unexpectedly. However, target mRNAs recognized by both miRNA and AUF1 are less abundant upon AUF1 overexpression implying that AUF1 is a decay-promoting factor influencing multiple steps in AGO2–miRNA-mediated mRNA decay. Our findings indicate that AUF1 functions in promoting miRNA-mediated mRNA decay globally.

INTRODUCTION

Mammalian mRNA degradation is mainly regulated by RNA-binding proteins (RBPs) and small non-coding RNAs including microRNAs (miRNAs) (1–3). The RBP AU-binding factor 1 (AUF1) has four isoforms: p37, p40, p42 and p45, and is implicated in cellular senescence, myogenesis, inflammation and cancer (4–6). The four isoforms bind similar RNA substrates with different affinities and have distinct subcellular localizations resulting in target mRNA decay (7). Recent transcriptome-wide analysis of AUF1 target RNAs revealed that AUF1 recognizes U-/GU- rich sequences in target transcripts and affects their stability either positively or negatively (8). Although the precise mechanism(s) by which AUF1 affects miRNA-mediated gene silencing is unknown, AUF1 may act as a complementary factor in AGO2–miRNA-mediated gene silencing by facilitating target mRNA recognition (9,10). AUF1 also directly regulates *DICER1* mRNA, leading repressor of miRNA biogenesis (11), which might be an output of negative feedback from increased mRNA degradation or translational repression by AUF1.

It was recently demonstrated that AUF1 directly binds a subset of mature miRNAs and transfers those miRNAs to AGO2 (12). miRNA loading onto AGO2 is enhanced in the presence of recombinant AUF1 *in vitro*, implying that AUF1 empowers AGO2-mediated mRNA degradation or selects specific miRNAs for loading on AGO2 in target mRNA degradation. These observations imply that AUF1 participates in miRNA-mediated gene silencing (9–11). However, it is not clear whether AUF1 is also involved in AGO2–miRNA-mediated gene silencing for mRNAs in global scale. Most studies focus on AGO2, limiting our knowledge of the function of AUF1 in gene silencing. Therefore, it is necessary to investigate AUF1's role in AGO2–miRNA-mediated gene silencing globally.

Single-molecule studies of human, mouse and *Drosophila* AGO2 revealed the dynamic nature of AGO2 for target mRNA recognition by seed base-paring (13–17). However, we cannot rule out that there is an alternative mode of target mRNA recognition by miRNAs beyond seed-matching mechanism. Correlations between miRNA and mRNA expression in steady state reveal that increased miRNA levels do not always lead to changes in the levels of all target mRNAs (18,19). It is important to identify additional features of target mRNA recognition by AGO2 at a given context. We examined the distance between seed-matched sites located within 3′ UTRs of mRNAs and AUF1 target sites on 3′ UTRs, revealing AUF1 binding sites on 3′ UTRs are found in close proximity to miRNA seed sites or even overlapped with miRNA binding sites (8), which could influence AGO2 binding on target mRNAs.

*To whom correspondence should be addressed. Tel: +1 843 792 8598; Fax: +1 843 792 8304; Email: yoonje@musc.edu
Correspondence may also be addressed to Sungchul Hohng. Tel: + 82 2 880 6593; Fax: +82 2 884 3002; Email: shohng@snu.ac.kr
†These authors contributed equally to the paper as first authors.

Here we report that AUF1 promotes AGO2 interactions with miRNA globally, however, it surprisingly delays the loading of AGO2 and miRNA to target mRNA recognized by AUF1, and decreases the abundance of AGO2 and let-7b target mRNAs. Our findings uncover a novel mechanism by which AUF1 promotes AGO2–miRNA-mediated selective mRNA decay.

MATERIALS AND METHODS

Cell culture, transfection, small interfering RNAs, microRNAs and plasmids

Human HeLa cells were cultured in Dulbecco's modified eagle's medium (Invitrogen) supplemented with 10% (v/v) Fetal Bovine Serum (FBS) and antibiotics. Cells were transfected (Lipofectamine 2000, Invitrogen) with siRNAs (20 nM) either *siControl* (UUCUCCGAACGUGUCACGUdTdT, targeting GFP), *siAUF1* (AAGAUCCUAUCACAGGGCGAUdTdT), or *siHuR* (CGUAAGUUAUUUCCUUUAAdTdT). Plasmids that expressed Flag-tagged AUF1 were described previously (20) and transfected at 1–2 μg [pcDNA, pcDNA–AUF1]. Cells were typically analyzed 48 h after transfection.

Western blot analysis

Whole-cell lysates, prepared in RadioImmunoPrecipitation Assay (RIPA) buffer, were separated by Sodium Dodecyl Sulphate-PolyAcrylamide Gel Electrophoresis (SDS-PAGE) and transferred onto nitrocellulose membranes (Invitrogen iBlot Stack). Primary antibodies recognizing HuR, Tubulin, and Actin were from Santa Cruz Biotechnology. The AUF1 antibody was from Millipore. AGO1, AGO2, AGO3 and AGO4 antibodies were from Abcam. Horse Radish Peroxidase (HRP)-conjugated secondary antibodies were from GE Healthcare.

RNP analysis

For immunoprecipitation (IP) of endogenous Ribonucleoprotein (RNP) complexes [RIP analysis (21,22)] from whole-cell extracts cells were lysed in 20 mM Tris–HCl at pH 7.5, 100 mM KCl, 5 mM $MgCl_2$ and 0.5% NP-40 for 10 min on ice and centrifuged at 10 000 × *g* for 15 min at 4°C. The supernatants were incubated with protein A-sepharose beads coated with antibodies that recognized AGO1, AGO2, AGO3, AGO4 (Abcam) or AUF1 (Millipore), or with control IgG (Santa Cruz Biotechnology) for 1 h at 4°C. After the beads were washed with NT2 buffer (50 mM Tris–HCl at pH 7.5, 150 mM NaCl, 1 mM $MgCl_2$ and 0.05% NP-40), the complexes were incubated with 20 units of RNase-free DNase I (15 min at 37°C) and further incubated with 0.1% SDS/0.5 mg/ml Proteinase K (15 min at 55°C) to remove DNA and proteins, respectively. The RNA isolated from the IP materials was further assessed by reverse transcription (RT)-quantitative polymerase chain reaction (qPCR) analysis using the primers listed (supplemental Table S4). Normalization of RIP results was carried out by quantifying in parallel the relative levels of *U6* snRNA in each IP sample. These abundant RNAs are non-specific contaminants present in the IP components (such as microfuge tube and beads).

RNA analysis

Trizol (Invitrogen) was used to extract total RNA and acidic phenol (Ambion) was used to extract RNA for RIP analysis (21,22). RT was performed using random hexamers and reverse transcriptase (Maxima, Thermo Scientific) and real-time, qPCR using gene-specific primers (Supplementary Table S1) and SYBR green master mix (Kapa Biosystems) using an Applied Biosystems 7300 instrument. miRNA quantitation was performed after RNA extraction from immunoprecipitated samples (with anti-AGO2 or control IgG), polyadenylation (System Biosciences QuantiMiR kit) and hybridization with oligo-dT adaptors. After RT, cDNAs were quantitated by qPCR with miRNA-specific primers or with primers to detect the control transcript *U6* snRNA, along with a universal primer.

Single-molecule Fluorescence Resonance Energy Transfer (FRET) assay

This study was performed based on modifications to a previously described method (23). Quartz slides and coverslips were cleaned in piranha solution (3:1 solution of concentrated sulfuric acid and 30% [v/v] hydrogen peroxide) for 20 min, and coated with 40:1 mixture of polyethylene glycol (MPEG-SVA-5000; Laysan Bio) and biotinylated polyethylene glycol (Biotin-PEG-SVA-5000; Laysan Bio). The flow cell was assembled by sandwiching double-sided sticky tape (3M) between a quartz slide and a cover slip. Polyethylene tubings (PE50; Becton Dickinson) were connected to inlet and outlet of the flow cell for stable buffer exchange during the fluorescence measurement. For the surface immobilization of target RNAs (Supplementary Table S1), streptavidin (0.2 mg/ml, Invitrogen) and target RNA (50 pM) were sequentially injected into the flow cell and incubated for 2 min. let-7b RNA (40 nM) was incubated with excessive human AGO2 (1 μM) at 23°C for 1 h to form AGO2–let-7b complex. Fluorescence measurement was carried out with imaging buffer (10 mM Tris [pH 8.0] with KCl [135 mM], $MgCl_2$ [1 mM], Trolox [1 mM; Sigma], glucose oxidase [1 mg/ml; Sigma], catalase [0.04 mg/ml; Sigma], glucose [0.4% (w/v); Sigma] and RNase inhibitor [2000 U/ml Promega]). Single-molecule fluorescence image was taken using a home-built prism-type total internal reflection fluorescence microscope equipped with an electron-multiplying charge-coupled device (EMCCD) camera (IXON DV597ECS-BV; Andor Technology) at a frame rate of 1 Hz (23) with alternating laser excitation. Temperature of the flow cell and solution for was maintained at 37°C via temperature control system (Live Cell Instruments).

miRNA sequencing

Briefly, in a total reaction volume of 20 μl, 2 μg total RNA was ligated to 100 pmol adenylated 3′ adapter containing a unique pentamer barcode (App- (Barcode)TCGTATGCCGTCTTCTGCTTGT), 1 μg Rnl2 (1–249) K227Q (plasmid for expression of recombinant ligase is available at www.addgene.org) in 50 mM Tris–HCl, pH 7.6, 10 mM $MgCl_2$, 10 mM 2-mercaptoethanol, 0.1 mg/ml acetylated bovine serum albumin (BSA) (Sigma, St Louis,

MO, USA) and 15% dimethyl sulfoxide (DMSO) for 16 h on ice. Following 3′ adapter ligation, 21 barcoded samples were pooled and products were purified on a 15% denaturing polyacylamide gel. Small RNAs, measuring 45–50 nt in length, were excised from the gel, eluted and ligated to 100 pmol 5′ oligoribonucleotide adapter (GUUC AGAGUUCUACAGUCCGACGAUC) in a 20 μl reaction volume using 1 μg T4 RNA ligase 1 (Rnl1) (Thermo Fisher, Glen Burnie, MD,USA) in 50 mM Tris–HCl, pH 7.6, 10 mM $MgCl_2$, 10 mM 2-mercaptoethanol, 0.1 mg/ml acetylated BSA, 0.2 mM adenosine triphosphate and 15% DMSO for 1 h at 37°C. Ligated small RNAs were purified on a 12% polyacrylamide gel, reverse transcribed using SuperScript III Reverse Transcriptase (Life Technologies, Carlsbad, CA, USA) and amplified by PCR using appropriate primers (forward primer: AATGATACGGCGACCA CCGACAGGTTCAGAGTTCTACAGTCCGA; reverse primer: CAAGCAGAAGACGGCATACGA). cDNA libraries were sequenced on an Illumina HiSeq 2000 instrument at the Rockefeller University Genomics Resource Center.

RESULTS

Previous reports of AUF1 and AGO2 (9,10) provide limited definitions of the general role of AUF1 in AGO2–miRNA-mediated mRNA translation repression/or decay due to targeted approached with selective mRNAs. Anisotropy of AUF1 and miRNAs *in vitro* showed that all isoforms of AUF1 bind to selective miRNAs containing UU- and UG-rich sequences with different affinities (12). This prompted us to utilize data from AUF1 Photoactivatable Ribonucleoside-Enhanced Crosslinking and Immunoprecipitation (PAR-CLIP) to investigate global function of AUF1 in miRNA-mediated gene silencing (Supplementary Figure S1A) (8), and we identified 14 miRNAs shared by all isoforms of AUF1. To determine whether capacity of AUF1 in miRNA binding influences miRNA-mediated gene silencing positively or negatively, we first investigated whether the binding of AGO2 to all miRNAs changes after AUF1 depletion. To this end, we employed AGO2 RIP-seq upon AUF1 depletion in HeLa.

Forty-eight hours after silencing AUF1 using small interfering (si)RNA, sequencing of miRNAs present in AGO2 IP material indicated that AUF1-target miRNAs (Supplementary Figure S1A) showed less binding to AGO2 when AUF1 was silenced (Figure 1A and Supplementary Table S2, $P < 2.2e^{-16}$, Kolmogorov–Smirnov test). For the normalization of miRNA sequencing, Fragments Per Kilobase of transcript per Million mapped reads (FPKM) of annotated miRNAs from AGO2 IP was divided by FPKM of miRNAs from total RNA after transfection of siRNAs targeting *GFP*, *AUF1* or *HuR* mRNA respectively. We checked siRNA efficiency using the same lysates to validate our AGO2 RIP and miRNA sequencing (Supplementary Figure S1B). When AUF1 is depleted more than 50% compared to control, miRNA–AGO2 interaction is similarly reduced in each experiment (Supplementary Figure S1C). HuR siRNA also depleted its protein level more than 50% compared to control (Supplementary Figure S1B), indicating differences observed in AUF1 and HuR knock-down are not due to differences in their siRNA efficiency. Moreover, either AUF1 or HuR knock-down did not affect AGO2 protein level and AGO2 IP efficiency was similar across different samples (Supplementary Figure S1B).

Decline in miRNA-AGO2 interaction did not reflect lower levels of these miRNAs in the cell after AUF1 silencing, since the levels of miRNAs in the IP samples were normalized to total miRNA levels in the corresponding 'input' materials. Thus, this data represents the relative enrichment of each miRNA compared to total expression level. We also performed RIP followed by RT-qPCR analysis as an independent measure to evaluate miRNAs enrichment in AUF1 IP material (Supplementary Figure S1C). In addition, HuR silencing did not have this robust effect (Figure 1B and Supplementary Table S2), indicating that the reduced binding of these miRNAs to AGO2 occurred specifically when AUF1 was silenced (Supplementary Table S2) and was unlikely to arise from non-specific loading of miRNAs onto AGO2. This result implies that each miRNA-binding protein has a distinct preference for its recognition of target miRNAs and may affect miRNA-mediated gene expression positively or negatively.

To further support our hypothesis, we compared the result of AGO2 RIP-seq with miRNAs identified from AUF1 PAR-CLIP. Globally, AUF1 silencing suppressed AGO2 interactions with AUF1-target miRNAs (defined as those containing >10 AGO2 RIP-seq reads) more severely than it suppressed AGO2 binding to miRNAs that were not AUF1 targets, as measured by RIP-seq analysis. This preferential suppression occurred when we considered all AUF1 isoforms together (Figure 2, 'ALL', top) or each isoform separately (Figure 2, bottom) with statistical significance ($P < 2.2e^{-16}$, Kolmogorov–Smirnov test). Our results support the notion that AUF1 facilitates the AGO2–miRNA interaction (12) and all AUF1 isoforms act as a complementary factor that promotes their target miRNA loading to AGO2.

We next tested whether AUF1 also influences miRNA loading onto other AGO family proteins. For this, we performed AGO RIP to determine enrichment of individual miRNAs in AGO1-4 IP material upon AUF1 depletion. We chose let-7b as a candidate miRNA since it is one of the target miRNAs recognized by all AUF1 isoforms. Interestingly, AGO2 and AGO3 were most affected by AUF1 depletion in their affinity to bind let-7b, but AGO1 and AGO4 were not (Supplementary Figure S1C) (24). Our results suggested that AUF1 might selectively promote AGO2 and AGO3–miRNA interactions.

Next we tested if the presence of AUF1 facilitates AGO2 and miRNA loading to target mRNA at a single-molecule level. Specifically, we measured the kinetics of AGO2 and let-7b loading to the immobilized *POLR2D* mRNA 3′ UTR fragment as performed previously (15,25). Two tether RNAs were tested: one with a let-7b site and the other with a let-7b site having seed-mutation to AUGGA (Figure 3A); both had a linker region to prevent steric hindrance. Using the tether RNA without AUF1 binding site, the binding rate to the AGO2–let-7b complex was unexpectedly decreased (42%) in the presence of AUF1 (p37) (100 nM) (Figure 3B and C). Addition of HuR did not change the loading rate (Figure 3D) and seed mutation blocked the assembly of AGO2–let-7b-POLR2D RNA completely (Figure 3E).

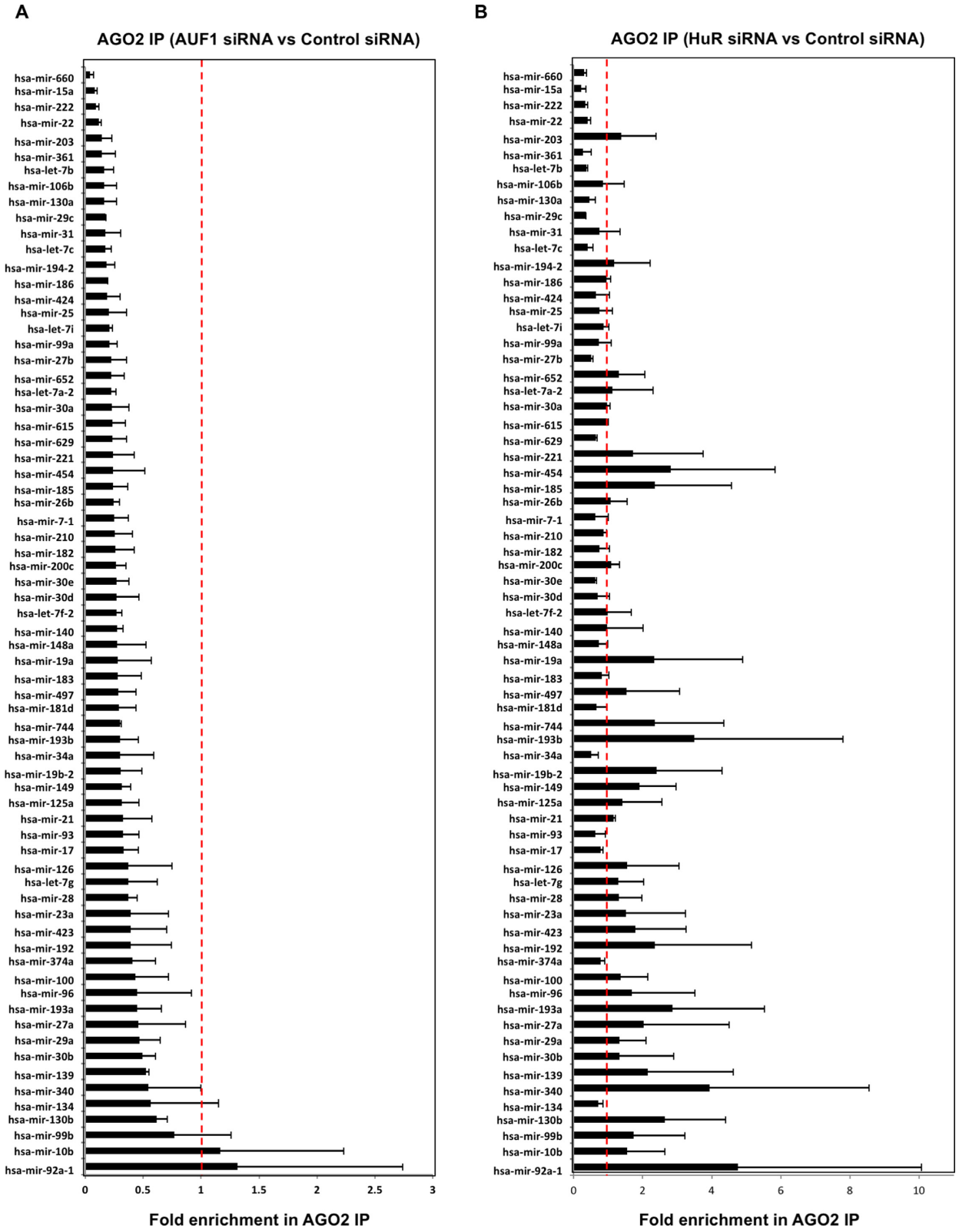

Figure 1. AU-binding factor (AUF)1 promotes AGO2–miRNA interactions. (**A** and **B**) Forty-eight hours after transfection of HeLa cells with AUF1-directed (A), HuR-directed (B) siRNA or Control siRNA, the relative abundance of miRNAs forming complexes with AGO2 was determined by RIP analysis followed by miRNA sequencing after normalization to input RNA. Data in graphs represent the means and Standard Deviation (S.D.) from two independent experiments.

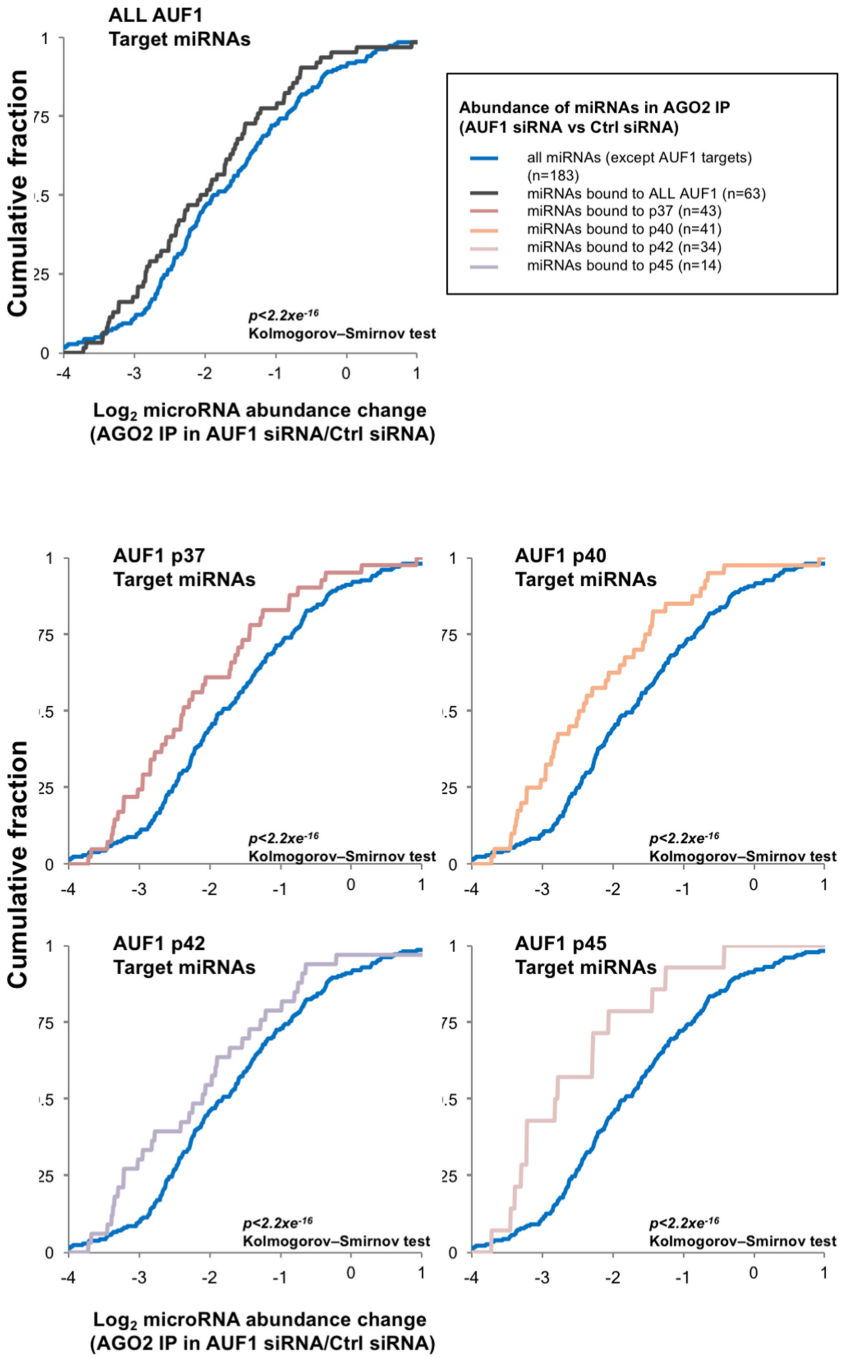

Figure 2. AUF1 selectively promotes target miRNAs interaction with AGO2. Cumulative plots of AGO2-bound miRNAs after AUF1 silencing; differences in binding of AGO2 to all miRNAs except AUF1 target miRNAs (*ALL*) as well as to miRNAs bound to each AUF1 isoform are indicated.

These results demonstrate that AUF1 slows down assembly of AGO2–let-7b-target RNA in single-molecule level.

We also tested target RNA with let-7b site and AUF1-binding region (Figure 4A). At this time, we also introduced mutation in seed-sequence and/or AUF1-binding region by randomization (Figure 4A). Our Fluorescence Resonance Energy Transfer (FRET) assay revealed that with the tether RNA that had both an AUF1 binding site and let-7b site, the binding was hindered more (78%) in the presence of AUF1 (100 nM) (Figure 4B and C). These results imply that AUF1 declines AGO2–miRNA-target–RNA assembly more strongly if the mRNA is also a AUF1 target (Figures 3 and 4C). Introduction of random sequence neither affected AGO2–let-7b assembly nor influenced the loading rate after addition of AUF1 or HuR (Figure 4D). In addition, mutation of UACCU to AUGGA in seed-sequence completely repressed assembly of AGO2–let-7b on target RNA (Figure 4E). These results indicate that AUF1 suppresses AGO2–let-7b-target RNA assembly further when it is bound to target RNAs and non-specific RNA-binding activity is not in-

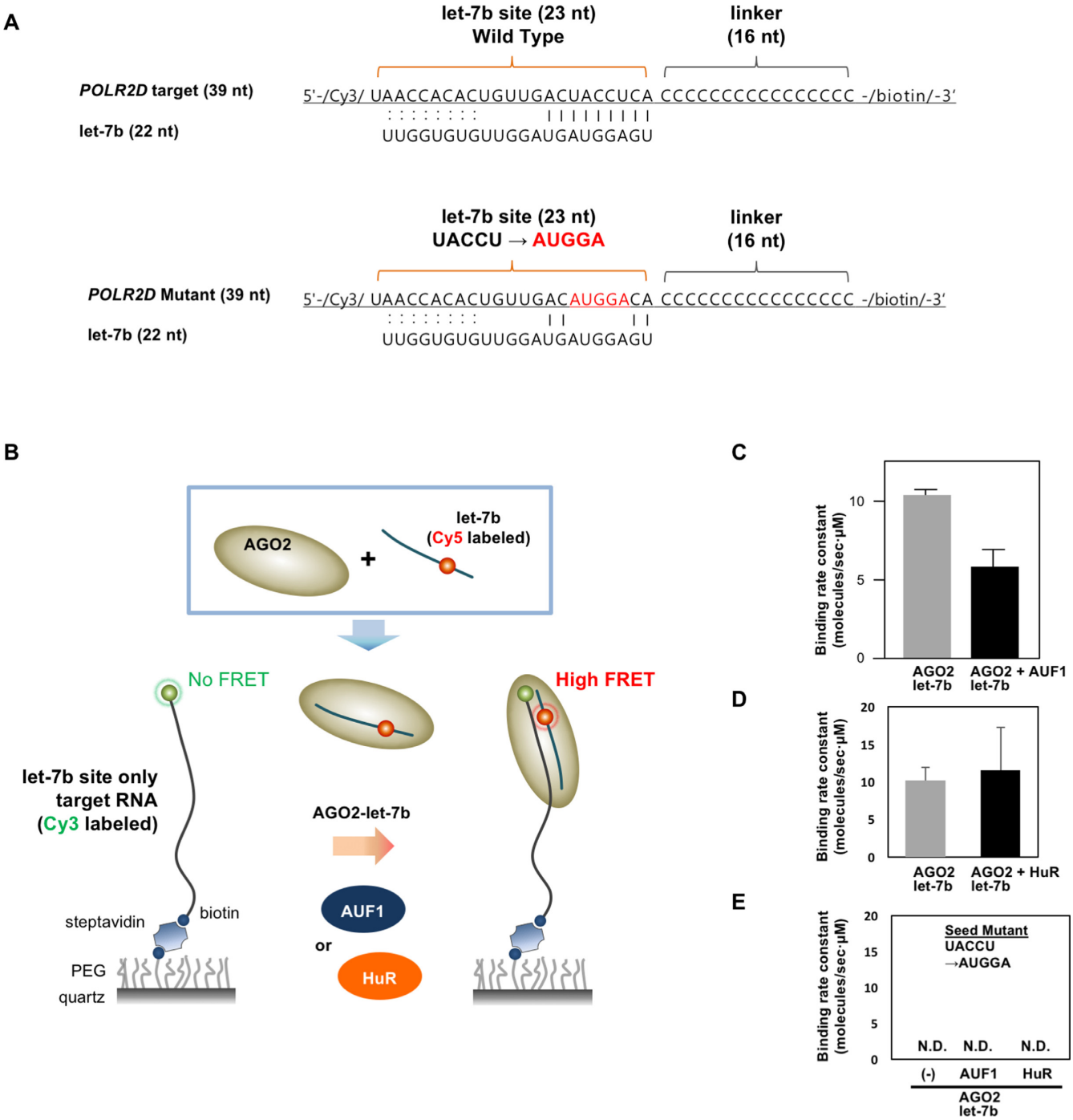

Figure 3. AUF1 slows down AGO2–let-7b:target RNA assembly. (**A**) Sequence of target mRNA construct containing let-7b and linker. 3′-end is biotinylated and 5′-end is labeled with Cy3 for POLR2D target. UACCU is mutated to AUGGA in seed-sequence. The 18_{th} Uracil of let-7b is labeled with Cy5. (**B** and **C**) Single-molecule FRET assay to determine the binding rate constant of AGO2–let-7b on target RNA bearing let-7b site only. (**D** and **E**) Single-molecule FRET assay with recombinant HuR or target RNA containing seed-mutation. N.D. indicates data with no detectible signal from FRET. Error bars represent S.D. from three independent measurements

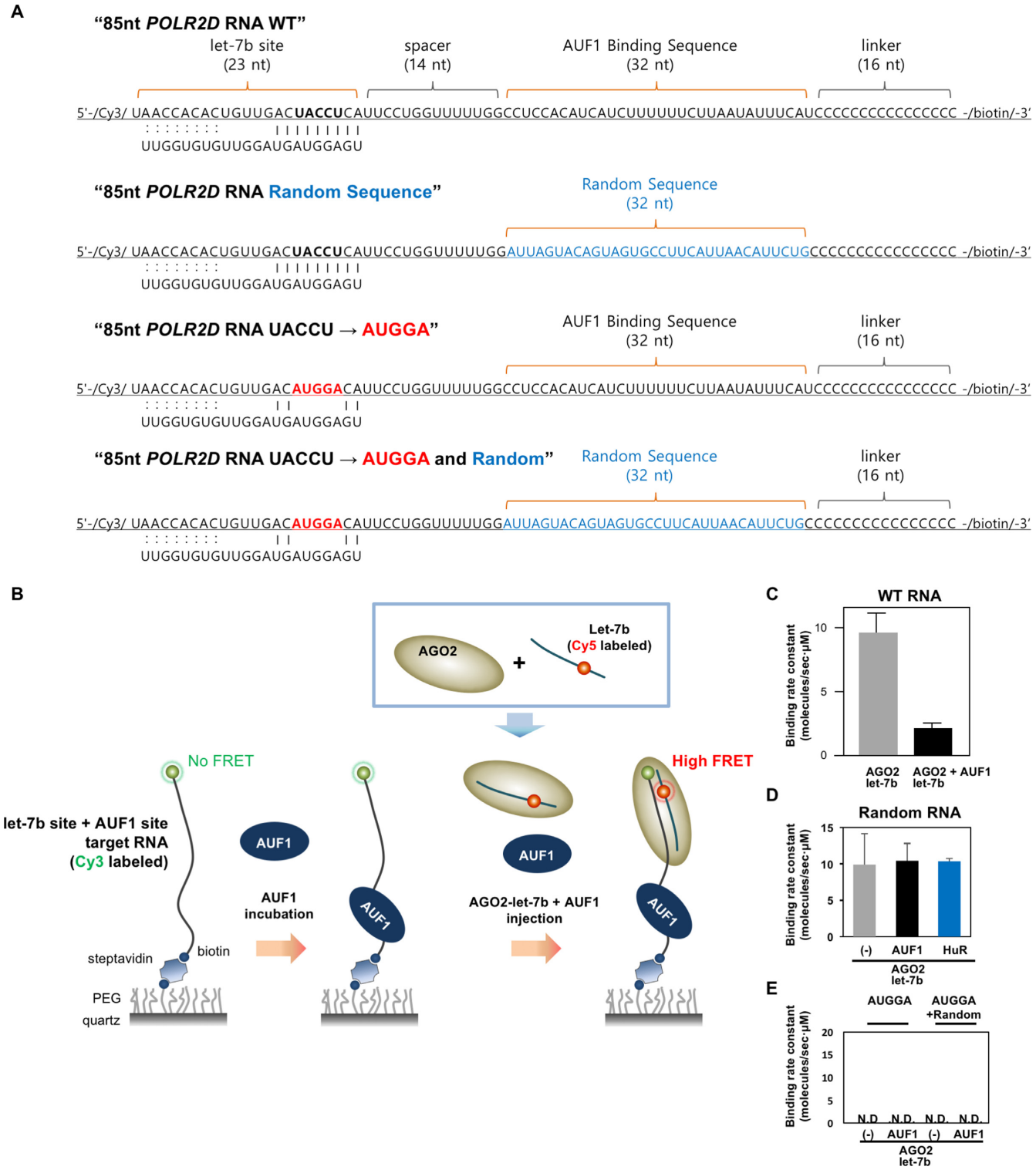

Figure 4. AUF1 represses assembly of AGO2–let-7b on target RNA containing AUF1-binding site. (**A**) Sequence of target mRNA construct containing let-7b, spacer, AUF1 site and linker. 3′ end is biotinylated and 5′ end is labeled with Cy3 for POLR2D target. AUGGA mutation is introduced in the seed-sequence and/or randomization of AUF1-binding sequence is performed. The 18_{th} Uracil of let-7b is labeled with Cy5. (**B** and **C**) Single-molecule FRET assay to determine the binding rate constant of AGO2–let-7b on target RNA bearing let-7b site and AUF1 binding site. AUF1 was pre-incubated before injecting AGO2–let-7b and AUF1. (**D** and **E**) Single-molecule FRET assay with seed-mutation and/or randomization of AUF1-binding sites in the presence of AUF1 or HuR. N.D. indicates data with no detectible signal from FRET. Error bars represent S.D. from three independent measurements

volved in AUF1-mediated repression of the complex assembly.

Importantly, these experiments (Figure 4) were performed in the presence of excess AUF1 p37 pre-bound to the immobilized tether RNA that imitates the case where AUF1 recognizes long RNAs more strongly than small RNAs. AUF1 PAR-CLIP data support this idea that binding sites are observed more in the region of mRNAs than small RNAs implying that AUF1 prefers a longer RNA substrate. Therefore, we conclude that AUF1 p37 slows down the loading rate of AGO2–let-7b to target RNA. However, this may not actually delay target RNA decay by miRNA in mammalian cells since the activity of AUF1 in facilitating miRNA loading to AGO2 (12) could offset the delay occurring in the intermediate step when AGO2–let-7b complex recognizes target RNA.

Inhibition of AGO2–let-7b loading to target RNA prompted us to test if AUF1 globally affects miRNA-mediated mRNA decay. We first assessed the distance between AUF1 sites (defined by PAR-CLIP), (8) and AGO sites (defined by PAR-CLIP), (26) on 3′ UTRs of AUF1 target mRNA (Figure 5A and Supplementary Table S3, $P < 1.1 \times 10^{-16}$, the hypergeometric test), suggesting that AUF1 binding sites on 3′ UTRs are found in close proximity to AGO binding sites. Based on the close proximity of these sites, we hypothesized that AUF1 might influence the abundance of both AGO2 and AUF1 target mRNAs on a transcriptome-wide scale. The abundance of AGO and AUF1 target mRNAs decreased when all isoforms or each isoform of AUF1 were overexpressed in HEK 293 cells (8) compared to non-target mRNAs (Figure 5B and Supplementary Figure S3).

Although AGO2 may bind directly to a small subset (<10%) of mRNAs independently of a miRNA (26), AGO2 generally binds mRNAs guided by a miRNA. We performed a similar analysis to determine the distance between AUF1 PAR-CLIP sites on target 3′ UTRs and neighboring miRNA seed sites (predicted from miRTCat), (27) which gave us a comprehensive view on AUF1's role in AGO2–miRNA-mediated gene silencing. Similarly, when the AUF1 and let-7 sites on 3′ UTR of AUF1 target mRNA were in close proximity (<50 nt) (Figure 5C and Supplementary Table S4, $P < 1.1 \times 10^{-16}$, the hypergeometric test) we observed a decrease of let-7 and AUF1 target mRNAs after AUF1 overexpression (Figure 5D and Supplementary Figure S4). To further support our observation, we performed RIP analysis after transfection of Firefly luciferase reporter containing *POLR2D* 3′ UTR (12), revealing that AUF1 silencing decreased the enrichment of reporter mRNA whereas the enrichment of mutant reporter lacking let-7b seed-sequence was not responsive on change of AUF1 level (Figure 5E). This implies that AGO2 might be working in concert with other miRNA-binding factors that might stabilize AGO2 binding to target mRNAs or surveil proper target RNA recognition by AGO2 at a given context. Taken together, our results demonstrate that AUF1 promotes miRNA-mediated global mRNA decay.

DISCUSSION

Our findings in this study indicate that AUF1 is required for the loading of AGO2 with a variety of miRNAs (Figure 1) preferentially with its target miRNAs (Figure 2), supporting the assertion that AUF1 is a master regulator of miRNA loading to AGO2. In contrast to our prediction, single-molecule data revealed that AUF1 slows down AGO2–let-7b loading to target RNA, as shown in *POLR2D mRNA* by single-molecule FRET-based tethering assay (Figures 3 and 4). A possible interpretation of our results is that AUF1 actually inhibits AGO2–miRNA–target mRNA assembly resulting in stabilization of target mRNAs. Previous report of transcription regulation by AUF1 in the nucleus could be a factor to influence the steady state abundance of miRNA target mRNAs (5).

However, considering our results that AUF1 overexpression mainly reduces the abundance of AGO2 and let-7b target mRNAs (Figure 5), a reduced assembly rate of AGO2–let-7b–target RNA complex represents yet-to-be understood functions of AUF1 in miRNA-mediated mRNA decay. It is possible that each miRNA-binding protein has a distinct role in miRNA-mediated gene silencing, and they may intervene during several steps in AGO2–miRNA-mediated gene silencing. This makes it difficult to draw solid conclusion from one side of observation. Reduced assembly of AGO2–miRNA–target mRNA (Figures 3 and 4) in conjunction with increased miRNA loading to AGO2 by AUF1 (12) could destabilize target mRNAs of miRNA and AUF1 selectively and accurately (Figure 5 and Supplementary Figure S2). Recent findings argue that AGO2 phosphorylation cycle regulates interaction of AGO2 and target mRNAs to maintain the global efficiency of miRNA-mediated gene silencing (28). They observed that AGO2 phosphorylation inhibits its binding to target mRNA but inactivation of AGO2 phosphorylation also impairs global miRNA-mediated silencing by reducing AGO2`s availability to silence additional targets. Their findings are in line with our observation that kinetic repression of AGO2–miRNA–mRNA assembly by AUF1 *in vitro* promotes target mRNA decay in mammalian cells. Thus, it is possible that once AGO2 could persist on target mRNAs longer than necessary, AUF1 can inhibit AGO2-miRNA-mRNA assembly to increase the active pool of AGO2 on a per-target basis or prevent mischievous AGO2's binding to targets. Based on this idea, the process reducing the assembly kinetics of AGO2–miRNA–mRNA complex can facilitate global miRNA-mediated mRNA decay.

One of the possible predictions is that AUF1 may have a surveillance function in miRNA-mediated mRNA decay. This model proposes that AUF1 licenses the proper assembly of AGO2–miRNA–target mRNA complex so that appropriate target mRNA decay can be accelerated by AUF1 (Figure 5F). Considering that mouse AGO2 dissociates rapidly from seed-matched targets (29), proper base-paring of miRNA and target mRNA is a key step in miRNA-mediated mRNA decay. In this regard, we propose the existence of multiple functions of AUF1 in miRNA-mediated gene silencing. Several RBPs are reported to bind mature miRNAs with different affinities (30–32). Further studies on miRNA-binding proteins should also examine if RBPs

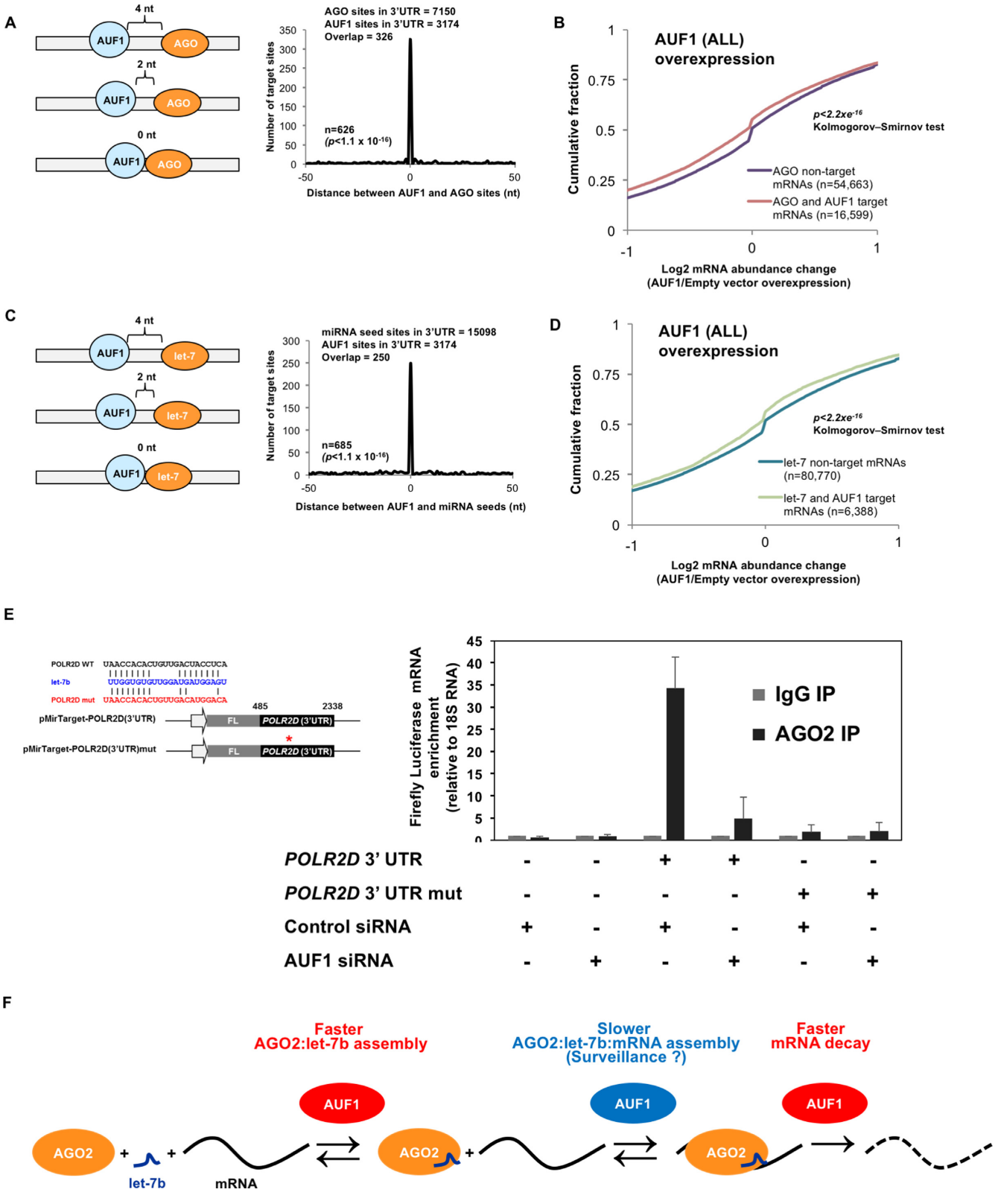

Figure 5. AUF1 globally decreases abundance of AGO and let-7 target mRNAs. (**A**) Number of AGO target sites (defined by PAR-CLIP) shared with AUF1 sites (defined by PAR-CLIP) on the 3′ UTRs of AUF1 target mRNAs within the distances indicated in the *x* axis; the analysis parameters, and *P*-value (using the hypergeometric test) are indicated. (**B**) Cumulative plots of AGO-target mRNAs (as identified by PAR-CLIP) after AUF1 overexpression. (**C**) Number of miRNA seed sites (predicted from miRTCat) (27), shared with AUF1 sites (defined by PAR-CLIP) on the 3′ UTRs of AUF1 target mRNAs within the distances indicated in the *x* axis; the analysis parameters and *P*-value (using the hypergeomtric test) are indicated. (**D**) Cumulative plots of predicted let-7 target mRNAs after AUF1 overexpression. (**E**) Forty-eight hours after transfecting HeLa cells with either wild-type or mutant reporter of *POLR2D* mRNA 3′ UTR with let-7b seed-mutation and the siRNA as indicated, the abundance of reporter (firefly luciferase) mRNAs from AGO2 RIP was assessed by RT-qPCR analysis. (**F**) Proposed model of AUF1 function in miRNA-mediated mRNA decay.

function as mRNA and/or miRNA binders impacting several stages of gene silencing to maximize the efficiency and fidelity of target mRNA decay.

SUPPLEMENTARY DATA

Supplementary Data are available at NAR Online.

ACKNOWLEDGEMENTS

We thank R. J. Schneider for providing reagents and information, J. A. Steitz for critical reading of the manuscript, and H. Markus for small RNA sequencing and analysis.
Author contributions: K.W.M., S.D., R.W.Z., S.K., L.L., J.H.Y., M.H.J. and S.S. designed and performed experiments. K.W.M., M.H.J., J.H.Y. and S.H. prepared the manuscript. The authors discussed the results and implications throughout.

FUNDING

Medical University of South Carolina Startup fund (to K.W.M., S.D., R.W.Z., L.L., J.H.Y.); NIA-IRP, NIH (to J.H.Y.); Creative Research Initiatives of the National Research Foundation of Korea [Physical Genetics Laboratory, 2009–0081562 to M.H.J., S.S., S.H.]. Funding for open access charge: Medical University of South Carolina Institutional Research (to J.H.Y., Principal Investigator).
Conflict of interest statement. None declared.

REFERENCES

1. Schoenberg,D.R. and Maquat,L.E. (2012) Regulation of cytoplasmic mRNA decay. *Nat. Rev. Genet.*, **13**, 246–259.
2. Fabian,M.R. and Sonenberg,N. (2012) The mechanics of miRNA-mediated gene silencing: a look under the hood of miRISC. *Nat. Struct. Mol. Biol.*, **19**, 586–593.
3. Wilczynska,A. and Bushell,M. (2015) The complexity of miRNA-mediated repression. *Cell Death Differ.*, **22**, 22–33.
4. Pont,A.R., Sadri,N., Hsiao,S.J., Smith,S. and Schneider,R.J. (2012) mRNA decay factor AUF1 maintains normal aging, telomere maintenance, and suppression of senescence by activation of telomerase transcription. *Mol. Cell*, **47**, 5–15.
5. Panda,A.C., Abdelmohsen,K., Yoon,J.-H., Martindale,J.L., Yang,X., Curtis,J., Mercken,E.M., Chenette,D.M., Zhang,Y., Schneider,R.J. *et al.* (2014) RNA-binding protein AUF1 promotes myogenesis by regulating MEF2C expression levels. *Mol. Cell. Biol.*, **34**, 3106–3119.
6. Moore,A.E., Chenette,D.M., Larkin,L.C. and Schneider,R.J. (2014) Physiological networks and disease functions of RNA-binding protein AUF1. *Wiley Interdiscip. Rev. RNA*, **5**, 549–564.
7. White,E.J.F., Brewer,G. and Wilson,G.M. (2013) Post-transcriptional control of gene expression by AUF1: Mechanisms, physiological targets, and regulation. *Biochim. Biophys. Acta*, **1829**, 680–688.
8. Yoon,J.-H., De,S., Srikantan,S., Abdelmohsen,K., Grammatikakis,I., Kim,J., Kim,K.M., Noh,J.H., White,E.J.F., Martindale,J.L. *et al.* (2014) PAR-CLIP analysis uncovers AUF1 impact on target RNA fate and genome integrity. *Nat. Commun.*, **5**, 5248.
9. Chang,N., Yi,J., Guo,G., Liu,X., Shang,Y., Tong,T., Cui,Q., Zhan,M., Gorospe,M. and Wang,W. (2010) HuR uses AUF1 as a cofactor to promote p16INK4 mRNA decay. *Mol. Cell. Biol.*, **30**, 3875–3886.
10. Wu,X., Chesoni,S., Rondeau,G., Tempesta,C., Patel,R., Charles,S., Daginawala,N., Zucconi,B.E., Kishor,A., Xu,G. *et al.* (2013) Combinatorial mRNA binding by AUF1 and Argonaute 2 controls decay of selected target mRNAs. *Nucleic Acids Res.*, **41**, 2644–2658.
11. Abdelmohsen,K., Tominaga-Yamanaka,K., Srikantan,S., Yoon,J.-H., Kang,M.-J. and Gorospe,M. (2012) RNA-binding protein AUF1 represses dicer expression. *Nucleic Acids Res.*, **40**, 11531–11544.
12. Yoon,J.-H., Jo,M.H., White,E.J.F., De,S., Hafner,M., Zucconi,B.E., Abdelmohsen,K., Martindale,J.L., Yang,X., Wood,W.H. *et al.* (2015) AUF1 promotes let-7b loading on Argonaute 2. *Genes Dev.*, **29**, 1599–1604.
13. Chandradoss,S.D., Schirle,N.T., Szczepaniak,M., MacRae,I.J. and Joo,C. (2015) A dynamic search process underlies microRNA targeting. *Cell*, **162**, 96–107.
14. Iwasaki,S., Sasaki,H.M., Sakaguchi,Y., Suzuki,T., Tadakuma,H. and Tomari,Y. (2015) Defining fundamental steps in the assembly of the Drosophila RNAi enzyme complex. *Nature*, **521**, 533–536.
15. Jo,M.H., Shin,S., Jung,S.-R., Kim,E., Song,J.-J. and Hohng,S. (2015) Human Argonaute 2 has diverse reaction pathways on target RNAs. *Mol. Cell*, **59**, 117–124.
16. Salomon,W.E., Jolly,S.M., Moore,M.J., Zamore,P.D. and Serebrov,V. (2015) Single-molecule imaging reveals that Argonaute reshapes the binding properties of its nucleic acid guides. *Cell*, **162**, 84–95.
17. Yao,C., Sasaki,H.M., Ueda,T., Tomari,Y. and Tadakuma,H. (2015) Single-molecule analysis of the target cleavage reaction by the Drosophila RNAi enzyme complex. *Mol. Cell*, **59**, 125–132.
18. Guo,H., Ingolia,N.T., Weissman,J.S. and Bartel,D.P. (2010) Mammalian microRNAs predominantly act to decrease target mRNA levels. *Nature*, **466**, 835–840.
19. Bazzini,A.A., Lee,M.T. and Giraldez,A.J. (2012) Ribosome profiling shows that miR-430 reduces translation before causing mRNA decay in zebrafish. *Science*, **336**, 233–237.
20. Sarkar,B., Xi,Q., He,C. and Schneider,R.J. (2003) Selective degradation of AU-Rich mRNAs promoted by the p37 AUF1 protein isoform. *Mol. Cell. Biol.*, **23**, 6685–6693.
21. Keene,J.D., Komisarow,J.M. and Friedersdorf,M.B. (2006) RIP-Chip: the isolation and identification of mRNAs, microRNAs and protein components of ribonucleoprotein complexes from cell extracts. *Nat. Protoc.*, **1**, 302–307.
22. Yoon,J.-H., Abdelmohsen,K., Srikantan,S., Yang,X., Martindale,J.L., De,S., Huarte,M., Zhan,M., Becker,K.G. and Gorospe,M. (2012) LincRNA-p21 suppresses target mRNA translation. *Mol. Cell*, **47**, 648–655.
23. Roy,R., Hohng,S. and Ha,T. (2008) A practical guide to single-molecule FRET. *Nat. Methods*, **5**, 507–516.
24. Yoon,J.-H., Srikantan,S. and Gorospe,M. (2012) MS2-TRAP (MS2-tagged RNA affinity purification): tagging RNA to identify associated miRNAs. *Methods*, **58**, 81–87.
25. Jung,S.-R., Kim,E., Hwang,W., Shin,S., Song,J.-J. and Hohng,S. (2013) Dynamic anchoring of the 3′-end of the guide strand controls the target dissociation of Argonaute–guide complex. *J. Am. Chem. Soc.*, **135**, 16865–16871.
26. Hafner,M., Landthaler,M., Burger,L., Khorshid,M., Hausser,J., Berninger,P., Ascano,M. Jr, Jungkamp,A.C., Munschauer,M., Ulrich,A. *et al.* (2010) Transcriptome-wide identification of RNA-binding protein and microRNA target sites by PAR-CLIP. *Cell*, **141**, 129–141.
27. Kim,K.-K., Ham,J. and Chi,S.W. (2013) miRTCat: a comprehensive map of human and mouse microRNA target sites including non-canonical nucleation bulges. *Bioinformatics*, **29**, 1898–1899.
28. Golden,R.J., Chen,B., Li,T., Braun,J., Manjunath,H., Chen,X., Wu,J., Schmid,V., Chang,T.-C., Kopp,F. *et al.* (2017) An Argonaute phosphorylation cycle promotes microRNA-mediated silencing. *Nature*, **542**, 197–202.
29. Wee,L.M., Flores-Jasso,C.F., Salomon,W.E. and Zamore,P.D. (2012) Argonaute divides its RNA guide into domains with distinct functions and RNA-binding properties. *Cell*, **151**, 1055–1067.
30. Yoon,J.-H., Abdelmohsen,K., Kim,J., Yang,X., Martindale,J.L., Tominaga-Yamanaka,K., White,E.J., Orjalo,A.V., Rinn,J.L., Kreft,S.G. *et al.* (2013) Scaffold function of long non-coding RNA HOTAIR in protein ubiquitination. *Nat. Commun.*, **4**, 2939.
31. Zealy,R.W., Wrenn,S.P., Davila,S., Min,K.W. and Yoon,J.H. (2017) microRNA-binding proteins: specificity and function. *Wiley Interdiscip. Rev. RNA*, **8**, doi:10.1002/wrna.1414.
32. Srivastava,M., Duan,G., Kershaw,N.J., Athanasopoulos,V., Yeo,J.H.C., Ose,T., Hu,D., Brown,S.H.J., Jergic,S., Patel,H.R. *et al.* (2015) Roquin binds microRNA-146a and Argonaute2 to regulate microRNA homeostasis. *Nat. Commun.*, **6**, 6253.